



Monosubstituted tricationic Zn(II) phthalocyanine enhances antimicrobial photodynamic inactivation (aPDI) of methicillin-resistant *Staphylococcus aureus* (MRSA) and cytotoxicity evaluation for topical applications: *in vitro* and *in vivo* study

Priyanga Dharmaratne ^{a*}, Baiyan Wang^{a*}, Roy C. H. Wong^{b*}, Ben C. L. Chan^c, Kit-Man Lau^c, Mei-Rong Ke^b, Clara B. S. Lau^c, Dennis K. P. Ng^b, Kwok-Pui Fung^{a,c,e} and Margaret Ip ^{d,f}

^aSchool of Biomedical Sciences, Faculty of Medicine, The Chinese University of Hong Kong, Hong Kong (SAR), People's Republic of China; ^bDepartment of Chemistry, Faculty of Science, The Chinese University of Hong Kong, Hong Kong (SAR), People's Republic of China; ^cInstitute of Chinese Medicine and State Key Laboratory of Research on Bioactivities and Clinical Applications of Medicinal Plants, The Chinese University of Hong Kong, Hong Kong (SAR), People's Republic of China; ^dDepartment of Microbiology, Faculty of Medicine, The Chinese University of Hong Kong, Prince of Wales Hospital, Hong Kong (SAR), People's Republic of China; ^eCUHK-Zhejiang University Joint Laboratory on Natural Products and Toxicology Research, Hong Kong (SAR), People's Republic of China; ^fShenzhen Research Institute, The Chinese University of Hong Kong, Shenzhen, People's Republic of China

ABSTRACT

Antimicrobial photodynamic therapy (aPDT) is an innovative approach to combat multi-drug resistant bacteria. It is known that cationic Zn(II) phthalocyanines (ZnPc) are effective in mediating aPDT against methicillin-resistant *Staphylococcus aureus* (MRSA). Here we used ZnPc-based photosensitizer named ZnPcE previously reported by our research group to evaluate its aPDT efficacy against broad spectrum of clinically relevant MRSA. Remarkably, *in vitro* anti-MRSA activity was achieved using near-infrared (NIR, >610 nm) light with minimal bactericidal concentrations ranging <0.019–0.156 μM against the panel of MRSA. ZnPcE was not only significantly ($p < .05$) more potent than methylene blue, which is a clinically approved photosensitizer but also demonstrated low cytotoxicity against human fibroblasts cell line (Hs-27) and human immortalized keratinocytes cell line (HaCaT). The toxicity was further evaluated on human 3-D skin constructs and found ZnPcE did not manifest *in vivo* skin irritation at $\leq 7.8 \mu\text{M}$ concentration. In the murine MRSA wound model, ZnPcE with PDT group demonstrated $> 4 \log_{10}$ CFU reduction and the value is significantly higher ($p < .05$) than all test groups except positive control. To conclude, results of present study provide a scientific basis for future clinical evaluation of ZnPcE-PDT on MRSA wound infection.

ARTICLE HISTORY Received 6 April 2020; Revised 23 June 2020; Accepted 28 June 2020

KEYWORDS Methicillin-resistant; *Staphylococcus aureus* (MRSA); antimicrobial photodynamic therapy (aPDT); phthalocyanine; murine wound infection model; cytotoxicity

Introduction

The development of bacterial resistance to available antibiotics is increasing at a very alarming rate globally [1]. This process is exacerbated by misuse and overuse of antibiotics both in humans and livestock. As a consequence, the last two decades have witnessed the emergence and spread of antibiotic resistance in pathogenic bacteria, and subsequently, the existing failed antibacterial treatment options have led to thousands of deaths annually [2].

Strains of *Staphylococcus aureus* (SA) that are resistant to all β -lactam antibiotics (with the exception of ceftaroline), known as methicillin-resistant SA (MRSA), were first identified among hospitalized

patients in 1960 [3]. MRSA is now endemic, and even epidemic, in many hospitals around the world, long-term care facilities [4], and communities [5]. With the increasing prevalence of MRSA, vancomycin was discovered to treat MRSA by inhibiting their cell wall synthesis. However, owing to the increasing use of vancomycin, vancomycin-resistant *S. aureus* (VRSA) has emerged, which further aggravates the problem of drug resistance [6]. Repeatedly, wherever antibiotics are used, antibiotic resistance will inevitably follow. Hence, scientists are motivated to find alternative ways to eradicate the multi-drug resistant (MDR) bacteria rather than the conventional use of antibiotics.

With a remarkably unique mode of action, antimicrobial photodynamic therapy (aPDT) has emerged

CONTACT Margaret Ip  margaretip@cuhk.edu.hk  Department of Microbiology, Faculty of Medicine, The Chinese University of Hong Kong, Prince of Wales Hospital, Sha Tin, New Territories, Hong Kong (SAR), People's Republic of China; Shenzhen Research Institute, The Chinese University of Hong Kong, Shenzhen, People's Republic of China

*Equal contributions in the research work

 Supplemental data for this article can be accessed <https://doi.org/10.1080/22221751.2020.1790305>

© 2020 The Author(s). Published by Informa UK Limited, trading as Taylor & Francis Group, on behalf of Shanghai Shangyixun Cultural Communication Co., Ltd
This is an Open Access article distributed under the terms of the Creative Commons Attribution-NonCommercial License (<http://creativecommons.org/licenses/by-nc/4.0/>), which permits unrestricted non-commercial use, distribution, and reproduction in any medium, provided the original work is properly cited.

as a promising alternative [7–9]. It utilizes the combined action of three nontoxic components, namely a photosensitizer (PS), light, and molecular oxygen to generate cytotoxic reactive oxygen species (ROS). aPDT provides significant advantages over the existing antimicrobial therapies. For example, resistant strains were equally susceptible as their naïve counterparts [10] or sometimes even more susceptible towards aPDT [11–13]. Secondly, the absence of toxicity towards non-irradiated tissues along with the high specificity of PS towards microorganism provides a perfect platform for the infected site-confined therapy. Consequently, toxicity is largely absent in the PS-depleted zone [14]. Finally, the rapid inactivation of microorganisms [15] as well as the limited or no resistance developed against the PSs has been reported to date [16,17].

Among the various classes of PSs being investigated [18–22], phthalocyanines are considered as PSs of particular interest due to the strong absorption they have at near infra-red region (ca.700 nm), allowing deep penetration, high efficiency in the generation of singlet oxygen, high photostability and easy chemical modification [23]. A number of structurally diverse phthalocyanines have been prepared and screened for their anti-MRSA activity *in vitro* [24–28] and *in vivo* [29–32]. Initial modifications of these phthalocyanines via D-glucopyranosyl substitution [26], Aluminium disulphonation or non-sulphonated compounds [24,25] only gave antibacterial activities at micromolar concentrations of these compounds [24–26]. These compounds tested were neutral in charge while subsequent studies revealed that substitutions of cationic moieties in the PS improved aPDT than neutral or negatively charged PSs [33–36]. This may be attributed to the fact that negatively charged thick peptidoglycan bi-layer has a greater affinity towards cationic PSs by facilitating the active transport of these compounds into the bacterial cells [37–39].

Our research group thus synthesized oligolysin-conjugated polycationic ZnPcs and tri-cationic monosubstituted ZnPcE (Figure 1) to study their aPDT activities against microbes including various bacterial, fungal and virus strains [26,27]. Indeed, all four ZnPcs yielded 4 log₁₀ CFU reductions *in vitro* at nanomolar concentrations against the MRSA ATCC BAA-43 strain, hence deserving a more comprehensive investigation with the best hit. In the current investigation, we determined the photodynamic minimal bactericidal concentration (PD-MBC) against a collection of clinically relevant MRSA (four ATCC type strains, two mutant strains and five each from representative hospital and community-acquired MRSA prevalent in Hong Kong and Southeast Asia), where the lethal dose at which bacterial eradication *in vitro* will be ascertained. Furthermore, none of the previous reports has studied the compatibility of the monosubstituted

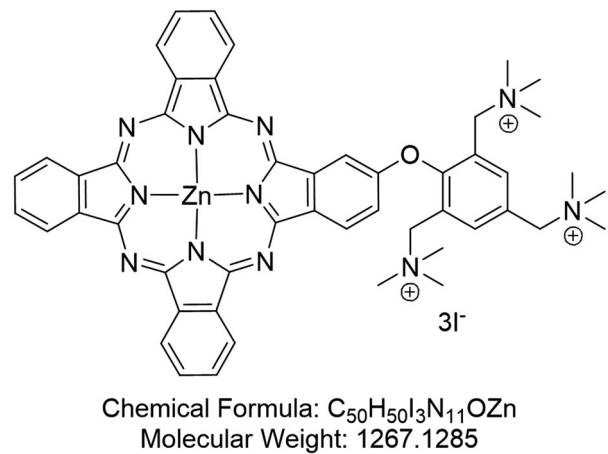


Figure 1. Chemical structure of ZnPcE.

ZnPcE compounds in mammalian systems. We thus examined the *in vitro* cytotoxicity of ZnPcE on human fibroblasts (Hs-27) and human immortalized keratinocytes (HaCaT). Additionally, an *in vivo* skin irritation assessment was also performed using human 3D skin constructs (EPI-200) to demonstrate its suitability for topical applications. Importantly, here we evaluated the efficacy of ZnPcE-PDT in an *in vivo* murine MRSA-infection full-thickness wound model to further support aPDT as a therapeutic modality for MRSA skin infection.

Materials and methods

Synthesis

ZnPcE was synthesized according to previously described method [24]. The reagents used were obtained from commercial sources and used as received unless otherwise noted.

Bacterial strains and culture conditions

The bacterial strains, MRSA (ATCC 43300, ATCC BAA-42, ATCC BAA-43, ATCC BAA-44) and two antibiotic-resistant SA strains, APH2''-AAC6' and RN4220/pUL5054, were included for testing. The APH2''-AAC6' strain expresses the bi-functional enzyme AAC(6')-APH(2''), which is an aminoglycoside-modifying enzyme conferring high-level gentamicin resistance (MIC: >128 µg/mL). The RN4220/pUL5054 strain over-expresses the *msr(A)* gene encoding for an ATP-binding cassette (ABC) transporter that induces resistance against erythromycin (MIC: 128 µg/mL) [40]. Ten non-duplicate clinical isolates, namely five hospital (HA)- and five community-associated (CA)-MRSA were included. They include important clonal types ST239, ST30, and ST59 previously documented to be prevalent in Hong Kong and in neighbouring countries [41–43]. All MRSA strains were grown in Mueller Hinton Broth (MHB) for 18 h at

37°C. The overnight culture suspension was adjusted to McFarland 0.5 and suspended in MHB to make a final concentration of 1.0×10^6 CFU/mL. Altogether, 16 MRSA strains (6 ATCC type strains and 10 clinical non-duplicate isolates) were included for *in vitro* aPDT studies.

***In vitro* photodynamic minimal bactericidal concentration (PD-MBC_{99.99%}) studies**

MBCs of ZnPcE and methylene blue (MB) were determined according to the Clinical and Laboratory Standards Institute (CLSI) guidelines [44] against sixteen strains in 96-well microtitre plates. Briefly, PS solution for PDT study was prepared freshly by dissolving ZnPcE in DMSO to make a 10 mM stock solution. It was then diluted in Tween 80 and MHB to set a desired stock solution. Serial two-fold dilutions procedure was employed to obtain final working concentrations. Tween 80 and DMSO concentrations were maintained $\leq 0.1\%$ and 1% (v/v), respectively. Aliquots of this suspension (200 μ L) were incubated in dark at 37°C for 120 min as pre-irradiation step. Selected plates were illuminated from above with light intensity 40 mW/cm² using a 300 W quartz-halogen lamp attenuated by a 5 cm layer of water (heat buffer) and a colour glass filter with a cut-on wavelength of 610 nm (65CGA-610, Newport, Franklin, MA, 176 USA) as shown in Section 1 in Supplementary information. The power densities were measured at multiple points where a 96 well plate was placed using a power metre with a thermal power sensor head (model S370C, 178 Thorlabs, Newton, New Jersey, USA) and noted to be comparable (~ 40 mW/cm²). The 96 well plate was illuminated for 20 min [26,27], corresponding to a fluence ($\lambda > 610$ nm) of 48 J/cm² for PDT. In order to evaluate the dark toxicity of ZnPcE, samples of each microbial suspension were incubated with ZnPcE separately and maintained in the dark for 140 min, corresponding to the pre-irradiation and illumination times. The effect of light alone was verified by adding 100 μ L of PBS to each microbial suspension, incubating it for 120 min and illuminating it for 20 min (48 J/cm²). The untreated control group (negative control) did not receive any PSs nor light. Solvent toxicity (blank control) also evaluated with 0.1% Tween 80 and 1% DMSO (v/v) to mimic *in vitro* aPDT assay. The positive control groups were incubated with varied concentrations of MB for 120 min followed by light illumination for 20 min. After the PDT, the plates were re-incubated at 37°C overnight under dark condition. To determine the MBC, the treated broth culture from wells which did not show any visible growth was cultured (10 μ L) on freshly prepared sterile blood agar plates. The least concentration (highest dilution) of the compound that completely inhibits colony formation on blood agar after incubation at 35°C

for 24 h was considered as MBC [45]. Each experiment was carried out in triplicate and the range of MBC values was reported.

***In vitro* cytotoxicity studies on Hs-27 and HaCaT cell line**

Human fibroblasts cell line (Hs-27) and human immortalized keratinocytes cell line (HaCaT) were used in this study. The procedure adopted for the cytotoxicity study was that of Woods et al. and Rusanov et al. [46,47]. These cell lines were maintained in Dulbecco's modified Eagle's medium (DMEM, Gibco, USA) supplemented with 10% (v/v) foetal bovine serum (FBS, Gibco, USA) and 1% (v/v) penicillin-streptomycin (full DMEM, Gibco, USA). The cells were incubated at 37°C in a humidified atmosphere of 5% CO₂ in the air. For the experiments, cells were detached from culture flasks with 0.25% trypsin-EDTA (Gibco, USA) incubated with Hs-27 and HaCaT for 2–3 and 15 min, respectively at 37°C.

The Hs-27 and HaCaT cells were seeded in 96-well plates (ThermoFisher Scientific, USA) to set 3×10^3 and 1×10^4 cells/well, respectively. Serial dilutions of MB and ZnPcE were added to the wells and incubated at 37°C for 120 min under dark conditions. The selective plates were irradiated with a light intensity of 40 mW/cm² for 20 min for PDT groups. The treated plates were re-incubated at 37°C for 48 h in dark. At the end of the incubation period, cell viability was determined by the 3-(4,5-dimethylthiazol-2-yl)-2,5-diphenyltetrazolium bromide (MTT) assay [48]. The optical density (OD) of each well was determined at 540 nm using a microplate reader (Bio-Tek Elx800, Winooski, VT). The toxicity represents the ratio of OD of a well in the presence of compounds to the OD of vehicle control wells in the presence of medium containing the corresponding percentage of DMSO.

***In vitro* EpiDerm™ skin irritation test (EPI-200-SIT)**

3D Human skin model

Reconstructed human three-dimensional skin constructs EpiDerm™ (EPI-200, MatTek Cor, Ashland, MA) were used for the toxicity test. This *in vitro* model consists of normal, human-derived epidermal keratinocytes (NHEK) cultured at the air-liquid interface on a semi-permeable tissue culture insert. The NHEK cells form a multilayered, highly differentiated model of the human epidermis that consists of organized basal, spinous, granular, and cornified layers (stratum corneum), closely resembling native human epidermis. The test was carried out according to the manufacturer's instructions. Method in briefly, upon arrival, the EpiDerm™ tissues were transferred to 6-well plates containing 0.9 mL maintenance media

provided with skin (MatTek Co. MA). Following 1 h pre-incubation, the tissues were then conditioned overnight at 37°C, 5% CO₂ in a humidified incubator.

Chemical exposure

Tissues were treated by topically applying 30 µL ZnPcE at a concentration of 0.78 µM (10× MBC) and 7.8 µM (100× MBC). For the negative and positive controls Dulbecco's phosphate-buffered saline (DPBS) and 5% sodium dodecyl sulphate (SDS) were used, respectively. All the test components were added and treated between 1 min intervals. Upon exposure of each test component for 60 ± 1 min, tissues were thoroughly washed with DPBS to remove residual test material. After which, transfer the blotted tissue inserts to a new 6 well-plate twice, containing 0.9 mL of fresh assay medium for 48 h incubation (transfer to fresh medium at time = 0 h after the wash and time = 24 h).

MTT tissue viability assay

EPI-200 tissue samples were washed twice with PBS and placed in a fresh 24-well plate containing 300 µL/well of 1 mg/mL MTT (MTT-100, MatTek Corporation) solution. After 3 h of incubation at 37°C, each insert was removed carefully, the bottom was blotted with paper wipes and the insert was transferred into a new 24-well plate. The culture inserts were then immersed in 2 mL/well of extraction solution (isopropanol). The plates were covered and incubated on a shaker for 2 h at room temperature in the dark. Inserts were discarded and the contents of each well were mixed thoroughly before transferring 200 µL of each sample into 96-well plates and the OD measured using the microplate reader at 540 nm. The % viability of the tissue was determined using the equation:

$$\% \text{ Viability} = 100 \times [\text{OD}_{(\text{sample})} / \text{OD}_{(\text{negative control})}].$$

Murine MRSA-infected wound model

A previously reported [28,49] murine skin infection model with modifications, was used to validate the *in vivo* efficacy of the ZnPcE-PDT treatment against MRSA. All animal experiments were conformed to the university guidelines and approved by the Animal Experimentation Ethics Committee (Ref. no.16/176/MIS) of The Chinese University of Hong Kong. 4–6 weeks old male BALB/c mice (17–21 g) were supplied by Laboratory Animal Services Centre (LASEC), The Chinese University of Hong Kong. They were housed in individual ventilated cages (IVC) under the conditions of 22–25°C and a 12 h light–dark cycle, with free access to chow and tap water. MRSA RN4220/pUL5054 was grown in MHB under aerobic conditions at 37°C with 100 rpm orbital shaking for overnight.

Table 1. Conditions of the five groups of mice in the murine MRSA wound infection aPDI model.

Group	No. of animals (n)	Treatment
A Negative control group (NC)	6	50 µL of distilled water alone
B Positive control group (PC)	6	50 µL of Fusidic cream alone
C Light control group (LC)	6	50 µL of distilled water + PDT
D Dark control group (DC)	6	50 µL of ZnPcE (7.8 µM) alone
E Test group (T)	6	50 µL of ZnPcE (7.8 µM) + PDT

The overnight culture was diluted with fresh MHB and re-incubated for 2–3 h until the mid-log growing phase. The desired suspension was centrifuged at 1000× g for 15 min to harvest the cell pallet. The cell pallet was re-suspended and diluted in MHB to achieve 0.6 optical density at 600 nm (OD₆₀₀) corresponded to 1 × 10⁸ CFU/mL, and used for wound inoculations.

On Day 0, mice were anaesthetized by an intraperitoneal (i.p.) injection of ketamine (40 mg/kg) and xylazine (8 mg/kg), with the hair of the back shaved, and the skin cleansed with 10% povidone-iodine solution. A circular full-thickness excision wound (4–5 mm in diameter) was established through puncher on the back subcutaneous tissue of each animal. The lesion overlaid with gauze was dressed up with adhesive bandage. Buprenorphine, commercially available as Temgesic®, at a dosage of 0.05 mg/kg was administered subcutaneously to the mice 12 hourly for 24 h after wound induction to relieve pain.

Two days after the wound induction (Day 2), mice were anaesthetized with ketamine/xylazine cocktail and in all animals, the adhesive bandage were removed. A 20 µL aliquot was drawn from the 1 × 10⁸ CFU/mL suspension of MRSA in MHB and spread evenly over the wound area using a micropipette. A dressing (Tegaderm™ film, 3M, USA) was applied to cover the wound immediately. The mice with infected wound were equally divided into five cohorts (n = 6 per each group) as listed in Table 1.

The first treatment was carried out 30 min after MRSA inoculation on Day 2. A 50 µL of 7.8 µM ZnPcE solutions, Fucidin (2% w/w) cream or distilled water was injected under the dressing (Tegaderm™ film) by syringe and allowed to spread over the wound.

For Group C and E, photoactivation (Biolitec group, Bonn, Germany) was initiated immediately. Single dosage of laser at 1W was delivered for 60 s by optical fibre 2 mm in diameter, corresponding to 60 J/wound. After each treatment, the mice were returned to IVC and Groups D and E were placed in dark. The second, third and fourth treatments were carried out on Day3, Day 5 and Day 9, respectively (Figure 2).

On Day 9, animals were killed with an overdose of dorminal pentobarbital solution after the last

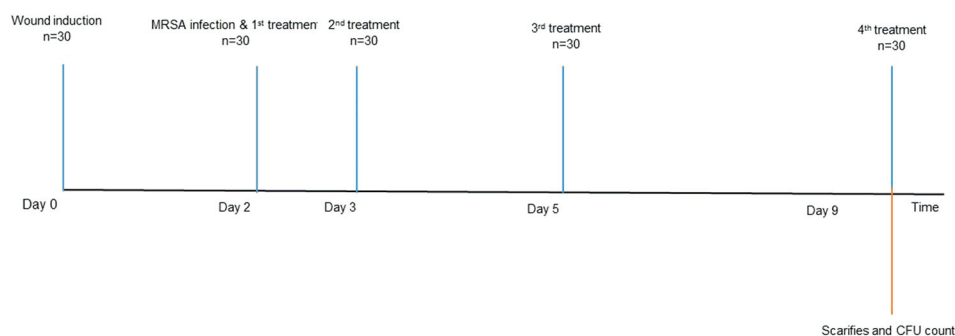


Figure 2. Timeline for *in vivo* aPDT study. Four treatment cycles were performed at Day 2, 3, 5 and 9. After the 4th treatment, the mice were sacrificed for the CFU count.

treatment. The wound (5 × 10 mm) was then excised aseptically. Each skin sample was homogenized in 0.5 mL of PBS solution for bacterial viability counts. Quantification of viable bacteria was performed by culturing serial dilutions (10 µL) of the bacterial suspension on blood agar plates. For this purpose, all plates were incubated at 37°C for 24 h and the bacteria counts in colony-forming units (CFU) were enumerated.

Results and discussion

In vitro PD-MBC_{99.99%} studies

ZnPcE was initially evaluated as a photosensitizer against a range of bacterial strains, including the Gram-positive methicillin-sensitive *S. aureus* (MSSA) ATCC 25923 and MRSA ATCC BAA-43, and the Gram-negative *Escherichia coli* ATCC 35218 and *Pseudomonas aeruginosa* ATCC 27853 by Ke et al. [26] by determining the CFU reduction. The photosensitizer concentration required to induce 4-log reduction of some of the bacterial strains was as low as 5 nM. The photosensitizer could also effectively inactivate some of the enveloped viruses. These preliminary studies showed that ZnPcE is a

promising photosensitizer for further investigation for aPDI.

In the current study, we determined complete eradication of ATCC type strains, mutant strains and clinically relevant MRSA (16 strains of *S. aureus*) to analyse the strain-dependent aPDI activity of ZnPcE and it resulted comparable anti-bacterial activity irrespective of their MDR status, sequence type or source of the strains. The aPDI of ZnPcE against MRSA are remarkably rapid and potent, by demonstrating complete eradication at concentration ranging from <0.019–0.156 µM (Table 2). In contrast, ZnPcE exhibited only modest bactericidal activity in the absence of light (5 to >10 µM concentration) (Table 2). The PDT effect thus increased the potency of ZnPcE against MRSA by over 2 log₁₀ when compared with its bactericidal activity in the dark (Table 2).

The aPDI of ZnPcE were compared with another PS exposed to similar λ_{max} value under identical conditions. MB, a mono-cationic phenothiazine, has been extensively studied and already in clinical use. *In vitro* aPDI studies using λ > 610 nm filter cut-on, light revealed that both PSs were active at this wavelength, but MB is significantly (*p* < .05) less potent

Table 2. The Minimal Bactericidal Concentrations (MBCs) values of ZnPcE and MB against 16 MRSA strains.

MRSA type	MRSA strain	ZnPcE			MB		
		PDT (µM)	No PDT (µM)	aPDI potency ^a	PDT (µM)	No PDT (µM)	aPDI potency
ATCC	43300	0.019–0.039	10	256–512	625	>2500 ^b	>4
ATCC	BAA 42	0.078	10	128	625	>2500	>4
ATCC	BAA 43	0.039–0.078	10	128–256	312.5–625	>2500	4->8
ATCC	BAA 44	0.078–0.156	10	64–128	312.5–625	>2500	4->8
Mutant	APH2AAC 6	0.156	5	32	625–1250	>2500	2->4
Mutant	RN4220	0.078	5	64	1250–2500	>2500	2->4
	/pUL5054						
CA ^c	W44	<0.019 ^d –0.019	>10 ^e	512–>512	2500	>2500	>1
CA	W45	0.019	>10	>512	1250–2500	>2500	1->2
CA	W46	0.019	>10	>512	2500	>2500	>1
CA	W47	0.019–0.039	>10	256–>512	2500	>2500	>1
CA	W48	0.039–0.078	>10	128–>256	2500	>2500	>1
HA ^f	W231	0.019–0.039	>10	256–>512	2500	>2500	>1
HA	W232	<0.019–0.019	>10	512–>512	2500	>2500	>1
HA	W233	0.019	>10	>512	2500	>2500	>1
HA	W234	0.019–0.039	>10	256–>512	2500	>2500	>1
HA	W235	<0.019–0.019	>10	512–>512	2500	>2500	>1

^aFold reduction in ZnPcE and MB concentration, relative to dark toxicity (no light exposure); ^bHighest concentration tested for MB; ^cCommunity-associated; ^dLowest concentration tested for ZnPcE; ^eHighest concentration tested for ZnPcE; ^fHospital-associated.

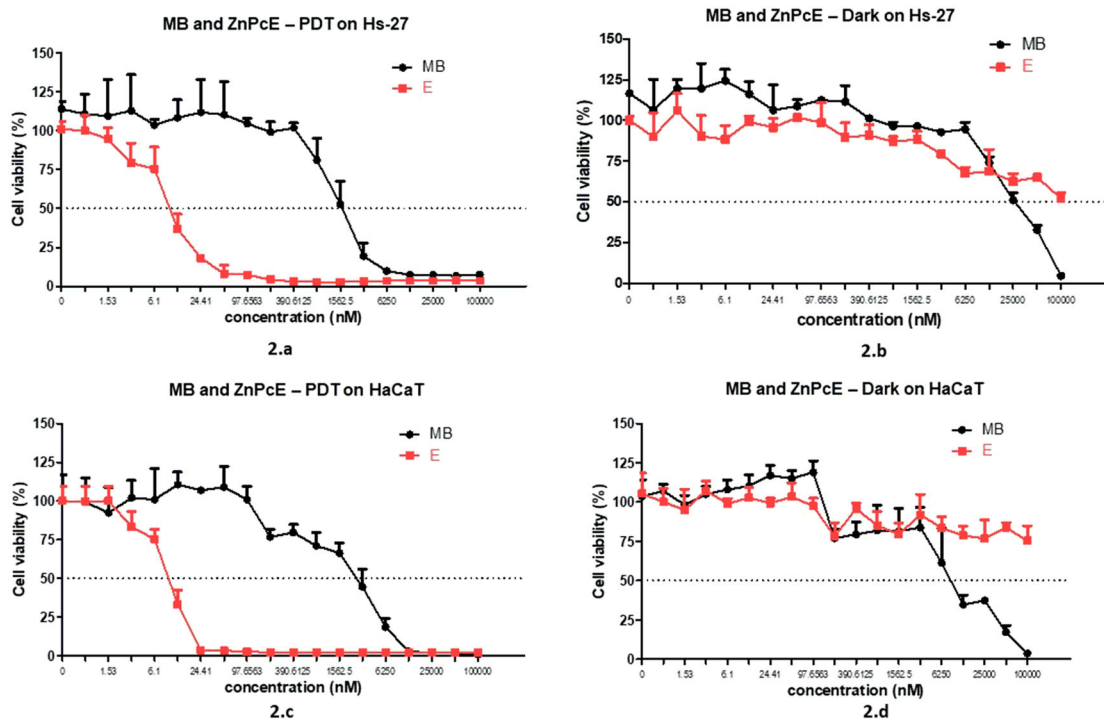


Figure 3. (a) Cytotoxicity of MB and ZnPcE on Hs-27 cells upon PDT ($n = 3$). (b) Cytotoxicity of MB and ZnPcE on Hs-27 cells under dark ($n = 3$). (c) Cytotoxicity of MB and ZnPcE on HaCaT cells upon PDT ($n = 3$). (d) Cytotoxicity of MB and ZnPcE on HaCaT cells under dark ($n = 3$). The LC_{50} values of ZnPcE against both Hs-27 and HaCaT is well above $100 \mu\text{M}$ and the values are significantly higher ($p < .05$) than MB under dark conditions.

than ZnPcE (Table 2). The difference of the aPDT potency may attribute to the higher cationic charge of ZnPcE (tri-cationic) than MB (mono-cationic), as well as due to the efficacy of the singlet oxygen formation ($\Phi_{\Delta} = 0.63$, respective to unsubstituted ZnPc) [26].

In vitro cytotoxicity studies on Hs-27 and HaCaT cell line

ZnPcE was tested for toxicity against Hs-27 and HaCaT cells to address potential effect for topical exposure with and without PDT. It is apparent from Figure 3(a) that upon irradiation, ZnPcE possessed significantly higher ($p < .05$) cytotoxicity than MB for Hs-27 cells. The cytotoxicity upon HaCaT also followed a similar pattern against ZnPcE (Figure 3(c)), implying the efficiency of ZnPcE in formation of ROS upon irradiation.

Furthermore, both Hs-27 and HaCaT cells were evaluated for dark toxicity following a 48-h incubation with double diluted concentration series of ZnPcE. The 50% lethal concentration (LC_{50}) values of ZnPcE under the dark condition were $>100,000 \text{ nM}$ for both cell lines and the values were significantly higher ($p < .05$) than the LC_{50} values of MB (Figure 3(b,d)). This cytotoxicity results suggested that the dark toxicities of ZnPcE against two normal cell lines are well above the concentration needed for complete eradication of the whole panel of MRSA (Table 2). We thus conclude that the ZnPcE-mediated aPDI is compatible with

mammalian systems under the conditions observed in the current investigation.

In vitro EpiDerm™ skin irritation test

The findings from *in vitro* cytotoxicity studies against Hs-27 and HaCaT cell lines prompted us to further investigate the effects of ZnPcE on human-derived non-transformed tissue model EpiDerm™. 3-D human skin culture (EpiDerm™) is a living reconstituted human epidermis used to provide information regarding cytotoxicity, irritant potential and immunotoxicity of different compounds [50].

As shown in Figure 4, the cell viability of EpiDerm™ cells after ZnPcE treatment at $0.78 \mu\text{M}$ (10 times of MBC value against MRSA RN 4220/pUL5054, ZnPcE-10) and $7.8 \mu\text{M}$ (100 times of MBC value against MRSA RN 4220/pUL5054, ZnPcE-100) were $85.41 \pm 4.3\%$ and $76 \pm 4.8\%$, respectively.

According to the manufacturer's instructions (Section 2 in supplementary information), ZnPcE did not manifest toxicity [according to the EU and GHS classification (R38/category 2 or no label)] on EpiDerm™ when $\leq 7.8 \mu\text{M}$ concentration. This finding supports the safe use of ZnPcE topically for aPDT.

Murine MRSA wound infection aPDI model

4-6-week-old male BALB/c mice were divided into five groups, each of six animals. The description of the five

Mean percentage cell viability of EPI-200 cells against ZnPcE at their different concentrations

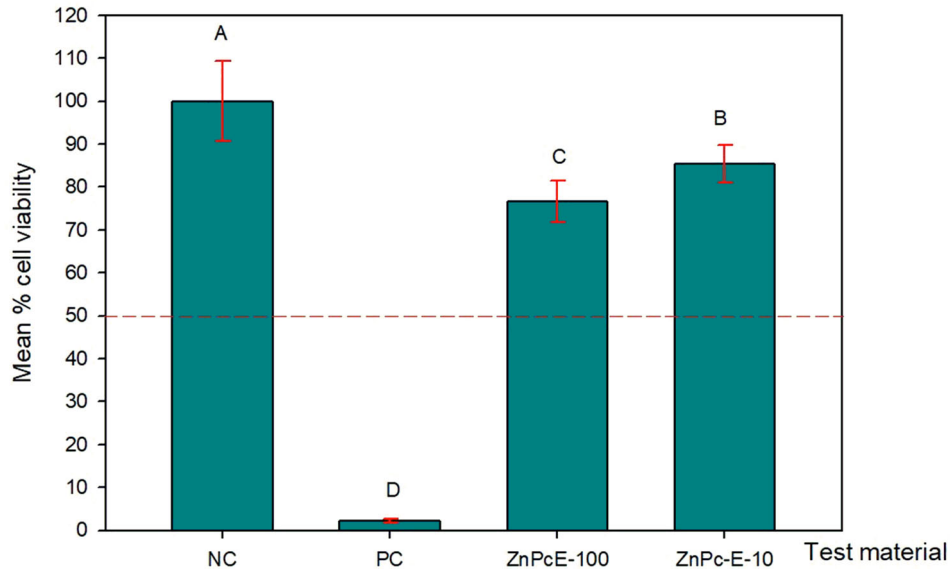


Figure 4. Cell viability of EPI-200 cells treated with DPBS [Negative control (NC)], 5% SDS [Positive control (PC)], 7.8 μM of ZnPcE [equivalent to $100 \times$ MBC against MRSA RN 4220/pUL5054 (ZnPcE-100)] and 0.78 μM of ZnPcE [equivalent to $10 \times$ MBC against MRSA RN 4220/pUL5054 (ZnPcE-10)]. Mean cell viability $> 50\%$ for the ZnPcE-100 and ZnPcE-10 implies ZnPcE did not pose any skin irritation for human 3-D skin construct at or below 7.8 μM concentration.

groups is given in Table 1. Full-thickness skin punch wounds (4–5 mm diameter) were introduced on animals and inoculated with MRSA RN4220/pUL5054. Compound treatments were added by direct application to infection sites. NIR ($\lambda > 610$ nm) was applied in four doses over nine days (Figure 2) with 60 s

irradiation in each treatment, and at day 9 the mouse was sacrificed and wound was dissected out for bacterial culture and enumeration of the CFU counts. The quantitative measures of bacterial load after four treatment cycles are given in Figure 5. In the light control group (Group C), the bacterial load decreased just

Bacterial load after 4 treatments (Day 9)

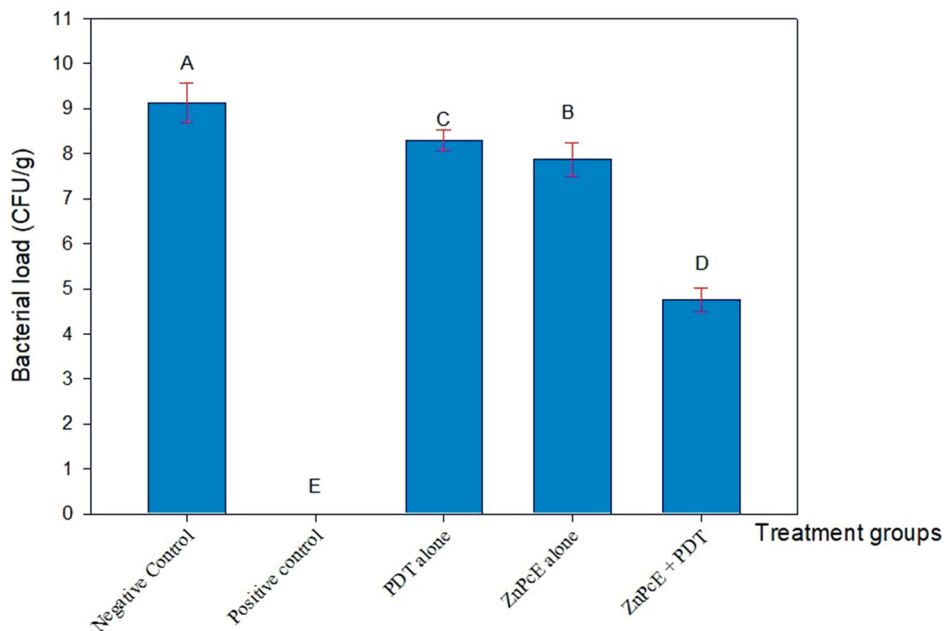


Figure 5. *In vivo* aPDT efficiency against MRSA RN4220/pUL5054 infected wound mediated by 7.8 μM concentration of ZnPcE. Experimental data are expressed as mean \pm SD ($n = 6$). Means that do not share a letter are significantly different. ZnPcE + PDT cohort showed significantly lower ($p < .05$) bacterial load after four treatment cycles, compared to all other treated groups, except positive control (2% Fusidic cream).

$0.83 \pm 0.23 \log_{10}$ CFU (Figure 5), confirming that the bacterial load was stable over four PDT cycles. For ZnPcE dark control (Group D), a $1.25 \pm 0.37 \log_{10}$ CFU reduction was observed (Figure 5). Application of light to the ZnPcE-treated cohort (Group E) demonstrated $4.36 \pm 0.27 \log_{10}$ CFU reduction which is significantly higher ($p < .05$) than all other cohorts, except positive control (Group E) that demonstrated complete eradication of bacteria (Figure 5). The *in vivo* aPDT activity of MRSA-infected wound in the current investigation showed comparatively higher activity than previous studies [30,31] on RLP068/Cl, a tetra-cationic ZnPc. Simonetti et al. [30] investigated RLP068/Cl mediated aPDT activity of a similar type of full thick MRSA-infected excision wound and observed only ≈ 2 logs reduction at day 9 of the infection. However, in this study, there were modifications with the wound establishment, since the wound induction and the bacterial inoculation both done on the same day and the treatment was started after 2 days of infection development. In the other study [31], aPDT activity was applied on an MRSA-infected scratch wound and 2.9 log unit decrease of bacterial bioluminescence was observed. Unlike our study, both RLP068/Cl mediated studies were performed with a single dose treatment but with significantly higher ($p < .05$) PS concentration and light dose.

The post-treatment monitoring of infection sites was performed after the final treatment by measuring the wound size and change in the body weight of animals. The size of negative control (Group A) wounds was slightly larger but there is no significant difference in wound size among the treatment groups. Furthermore, there is no body weight loss in the treatment groups when compared with the negative control (Group A) (Section 3 and 4 in supplementary information).

Conclusions

The tricationic ZnPcE being investigated in the study demonstrated high *in vitro* aPDI (MBC values ranging from <0.019 - $0.156 \mu\text{M}$) against the tested panel of MRSA with 2 \log_{10} potentiation upon irradiation. Furthermore, the comparable MBC values shown for the panel of MRSA strains suggested the possibility of using ZnPcE to treat *S. aureus* infections, regardless of their MDR status.

ZnPcE appeared to be nontoxic towards Hs-27 and HaCaT cells by demonstrating significantly higher ($p < .05$) LC_{50} values than the concentration needed for complete eradication (MBC value) of MRSA under this investigation. In addition, ZnPcE did not manifest any toxicity towards human 3-D skin constructs EpiDermTM even up to 2 \log_{10} of increase from the MBC value of RN4220/pUL5054. We thus conclude

that the ZnPcE-mediated aPDI is safe and compatible with mammalian systems.

In the *in vivo* studies in a murine MRSA wound infection model, ZnPcE with NIR irradiation demonstrated $> 4 \log_{10}$ CFU reduction which is significantly higher ($p > .05$) than all other test groups except for the positive control (2% Fusidic cream).

Optimization of the dose and dosing intervals of ZnPcE and the irradiation durations may further improve the treatment outcome. ZnPcE-PDT is a promising PDT compound with activity against MRSA infections and deserves further clinical investigations.

Author contributions

PD: Completed *in vitro* aPDT studies, completed skin irritation test using EpiDermTM, helped to perform *in vivo* aPDT studies and drafted the manuscript. **BY:** Designed and completed *in vitro* cytotoxicity studies and revised the manuscript. **RW and MRK:** Synthesized ZnPcE, evaluated the photo-physical data and revised the manuscript. **BCLC:** Designed and performed *in vivo* aPDT studies, and revised the manuscript. **KML:** Designed and performed *in vivo* aPDT studies, and revised the manuscript. **CBSL:** Commented on the study and revised the manuscript. **DKPN:** Advised on the synthesis of ZnPcE and provided critical feedback on the manuscript. **KPF and MIP:** Conceptualized, initiated, and oversaw the project.

Abbreviations

aPDI: Antimicrobial photodynamic inhibition; aPDT: Antimicrobial photodynamic therapy; ATCC: American Type culture collection; CA: Community associated; CFU: colony forming unit; DMEM: Dulbecco's minimum essential medium; DMSO: dimethyl sulfoxide; ESBL: extended spectrum β -lactamase; HA: Hospital associated; LC_{50} : 50% Lethal concentration; MB: Methylene blue; MBC: minimum bactericidal concentration; MDR: multi-drug resistant; MHB: Mueller Hinton broth; MRSA: methicillin-resistant *Staphylococcus aureus*; MSSA: methicillin-sensitive *Staphylococcus aureus*; PS: Photosensitizer; ROS: Reactive oxygen species; ST: Sequential type; VRSA: vancomycin-resistant *S. aureus*; ZnPc: Zn (II) phthalocyanines.

Disclosure statement

No potential conflict of interest was reported by the author(s).

Funding

This work was partially supported by a grant from Health and Medical Research Fund (HMRF 16151202), and by the Si Yuan Foundation, HKSAR, China.

Data availability statements

The authors confirm that the data supporting the findings of this study are available within the article [and/or] its supplementary materials.

ORCID

Priyanga Dharmaratne  <http://orcid.org/0000-0002-2084-0643>

Margaret Ip  <http://orcid.org/0000-0003-1291-6537>

References

- Levy SB, Marshall B. Antibacterial resistance worldwide: causes, challenges and responses. *Nat Med*. 2004;10; doi:10.1038/nm1145.
- Palmer AC, Kishony R. Understanding, predicting and manipulating the genotypic evolution of antibiotic resistance. *Nat Rev Genet*. 2013;14:243–248.
- Jevons MP. “Celbenin”-resistant Staphylococci. *Br Med J*. 1961;1(2):113–114. doi:10.1136/bmj.1.5219.113.
- Strausbaugh LJ, Crossley KB, Nurse BA, et al. Antimicrobial resistance in long-term-care facilities. *Infect Control Hosp Epidemiol*. 1996;17:129–140.
- Crum NF, Lee RU, Thornton SA, et al. Fifteen-year study of the changing epidemiology of methicillin-resistant *Staphylococcus aureus*. *Am J Med*. 2006;119:943–995. doi:10.1016/j.amjmed.2006.01.004.
- Hessling B, Bonn F, Otto A, et al. Global proteome analysis of vancomycin stress in *Staphylococcus aureus*. *Int J Med Microbiol*. 2013;303:624–634.
- Jori G, Fabris C, Soncin M, et al. Photodynamic therapy in the treatment of microbial infections: basic principles and perspective applications. *Lasers Surg Med*. 2006;38:468–481.
- Maisch T. A new strategy to destroy antibiotic resistant microorganisms: antimicrobial photodynamic treatment. *Mini Rev Med Chem*. 2009;9:974–983.
- Dharmaratne P, Sapugahawatte DN, Wang B, et al. Contemporary approaches and future perspectives of antibacterial photodynamic therapy (aPDT) against methicillin-resistant *Staphylococcus aureus* (MRSA): a systematic review. *Eur J Med Chem*. 2020;200:112341.
- Usacheva MN, Teichert MC, Biel MA. Comparison of the methylene blue and toluidine blue photobactericidal efficacy against gram-positive and gram-negative microorganisms. *Lasers Surg Med*. 2001;29:165–173.
- Wainwright M, Crossley K. Methylene blue – a therapeutic dye for all seasons? *J Chemother*. 2002;14:431–443.
- Topaloglu N, Gulsoy M, Yuksel S. Antimicrobial photodynamic therapy of resistant bacterial strains by indocyanine green and 809-nm diode laser. *Photomed Laser Surg*. 2013;31:155–162.
- Grinholc M, Szramka B, Kurlenda J, et al. Bactericidal effect of photodynamic inactivation against methicillin-resistant and methicillin-susceptible *Staphylococcus aureus* is strain-dependent. *J Photochem Photobiol B*. 2008;90:57–63.
- Liu Y, Qin R, Zaat SAJ, et al. Antibacterial photodynamic therapy: overview of a promising approach to fight antibiotic-resistant bacterial infections. *J Clin Transl Res*. 2015. doi:10.18053/jctres.201503.002.
- Dai T, Tegos GP, Zhiyentayev T, et al. Photodynamic therapy for methicillin-resistant *Staphylococcus aureus* infection in a mouse skin abrasion model. *Lasers Surg Med*. 2010;42:38–44. doi:10.1002/lsm.20887.
- Bartolomeu M, Rocha S, Cunha A, et al. Effect of photodynamic therapy on the virulence factors of *Staphylococcus aureus*. *Front Microbiol*. 2016;7:22–31. doi:10.3389/fmicb.2016.00267.
- Lauro FM, Pretto P, Covolo L, et al. Photoinactivation of bacterial strains involved in periodontal diseases sensitized by porphycene–polylysine conjugates. *Photochem Photobiol Sci*. 2002;1:468–470.
- Carpenter B, Situ X, Scholle F, et al. Antiviral, antifungal and antibacterial activities of a BODIPY-based photosensitizer. *Molecules*. 2015;20:10604–10621.
- Fekrazad R, Zare H, Vand SMS. Photodynamic therapy effect on cell growth inhibition induced by radachlorin and toluidine blue O on *Staphylococcus aureus* and *Escherichia coli*: an in vitro study. *Photodiag Photodyn Ther*. 2016;15:213–217.
- Meng S, Xu Z, Hong G, et al. Synthesis, characterization and in vitro photodynamic antimicrobial activity of basic amino acid–porphyrin conjugates. *Eur J Med Chem*. 2015;92:35–48.
- Darabpour E, Kashef N, Mashayekhan S. Chitosan nanoparticles enhance the efficiency of methylene blue-mediated antimicrobial photodynamic inactivation of bacterial biofilms: An in vitro study. *Photodiag Photodyn Ther*. 2016;14:211–217.
- Goto B, Iriuchishima T, Horaguchi T, et al. Therapeutic effect of photodynamic therapy using Na-pheophorbide a on osteomyelitis models in rats. *Photomed Laser Surg*. 2011;29:183–189.
- Sekkat N, Bergh HVD, Nyokong T, et al. Like a bolt from the blue: phthalocyanines in biomedical optics. *Molecules*. 2011;17:98–144.
- Griffiths M. Killing of methicillin-resistant *Staphylococcus aureus* in vitro using aluminium disulphonated phthalocyanine, a light-activated antimicrobial agent. *J Antimicrob Chemother*. 1997;40:873–876.
- Ribeiro APD, Andrade MC, Bagnato VS, et al. Antimicrobial photodynamic therapy against pathogenic bacterial suspensions and biofilms using chloro-aluminum phthalocyanine encapsulated in nanoemulsions. *Lasers Med Sci*. 2013;30:549–559.
- Ke M-R, Eastel JM, Ngai KL, et al. Photodynamic inactivation of bacteria and viruses using two monosubstituted zinc(II) phthalocyanines. *Eur J Med Chem*. 2014;84:278–283.
- Ke M-R, Eastel JM, Ngai KLK, et al. Oligolysine-conjugated zinc(II) phthalocyanines as efficient photosensitizers for antimicrobial photodynamic therapy. *Chem – An Asian J*. 2014;9:1868–1875.
- Zhao Z, Li Y, Meng S, et al. Susceptibility of methicillin-resistant *Staphylococcus aureus* to photodynamic antimicrobial chemotherapy with α -d-galactopyranosyl zinc phthalocyanines: in vitro study. *Lasers Med Sci*. 2013;29:1131–1138.
- Soncin M, Fabris C, Busetti A, et al. Approaches to selectivity in the Zn(ii)-phthalocyanine-photosensitized inactivation of wild-type and antibiotic-resistant

- Staphylococcus aureus*. Photochem Photobiol Sci. 2002;1:815–819.
- [30] Simonetti O, Cirioni O, Orlando F, et al. Effectiveness of antimicrobial photodynamic therapy with a single treatment of RLP068/Cl in an experimental model of *Staphylococcus aureus* wound infection. Br J Dermatol. 2011;164:987–995.
- [31] Vecchio D, Dai T, Huang L, et al. Antimicrobial photodynamic therapy with RLP068 kills methicillin-resistant *Staphylococcus aureus* and improves wound healing in a mouse model of infected skin abrasion PDT with RLP068/Cl in infected mouse skin abrasion. J Biophoton. 2012;6:733–742.
- [32] Li S, Cui S, Yin D, et al. Dual antibacterial activities of a chitosan-modified upconversion photodynamic therapy system against drug-resistant bacteria in deep tissue. Nanoscale. 2017;9:3912–3924.
- [33] Caruso E, Banfi S, Barbieri P, et al. Synthesis and antibacterial activity of novel cationic BODIPY photosensitizers. J Photochem Photobiol B. 2012;114:44–51.
- [34] Hamblin MR, Dai T. Can surgical site infections be treated by photodynamic therapy? Photodiag Photodyn Ther. 2010;7:134–136.
- [35] Morales-De-Echegaray AV, Maltais TR, Lin L, et al. Rapid uptake and photodynamic inactivation of Staphylococci by Ga(III)-Protoporphyrin IX. ACS Infect Dis. 2018;4:1564–1573.
- [36] Maisch T, Spannberger F, Regensburger J, et al. Fast and effective: intense pulse light photodynamic inactivation of bacteria. J Ind Microbiol Biotechnol. 2012;39:1013–1021.
- [37] Street CN, Pedigo LA, Loebel NG. Energy dose parameters affect antimicrobial photodynamic therapy-mediated eradication of periopathogenic biofilm and planktonic cultures. Photomed Laser Surg. 2010;28. doi:10.1089/pho.2009.2622.
- [38] Tang H, Yow CM, Hamblin MR. A comparative in vitro photoinactivation study of clinical isolates of multidrug-resistant pathogens. J Infect Chemother. 2007;13:87–91.
- [39] Mantareva V, Kussovski V, Angelov I, et al. Photodynamic activity of water-soluble phthalocyanine zinc(II) complexes against pathogenic microorganisms. Bioorg Med Chem. 2007;15:4829–4835.
- [40] Ross JI, Eady EA, Cove JH, et al. Inducible erythromycin resistance in staphylococci is encoded by a member of the ATP-binding transport super-gene family. Mol Microbiol. 1990;4:1207–1214.
- [41] Ip M, Yung RWH, Ng TK, et al. Contemporary methicillin-resistant *Staphylococcus aureus* Clones in Hong Kong. J Clin Microbiol. 2005;43:5069–5073.
- [42] Li J, Wang L, Ip M, et al. Molecular and clinical characteristics of clonal complex 59 methicillin-resistant *Staphylococcus aureus* infections in Mainland China. Plos One. 2013;8; doi:10.1371/journal.pone.0070602.
- [43] Wong J, Ip M, Tang A, et al. Prevalence and risk factors of community-associated methicillin-resistant *Staphylococcus aureus* (CA-MRSA) carriage in Asia-Pacific region from 2000 to 2016: a systematic review and meta-analysis. Int J Infect Dis. 2018;73:135–136.
- [44] Clinical and Laboratory Standards Institute (CLSI). Performance standards for antimicrobial susceptibility testing. 29th ed. Wayne (PA): CLSI supplement M100. Clinical and Laboratory Standards Institute; 2019.
- [45] Talib W, Mahasneh A. Antimicrobial, cytotoxicity and phytochemical screening of Jordanian plants used in traditional medicine. Molecules. 2010;15:1811–1824.
- [46] Woods JA, Traynor NJ, Brancalione L, et al. The effect of photofrin on DNA strand breaks and base oxidation in HaCaT keratinocytes: a comet assay study. Photochem Photobiol. 2004;79:105.
- [47] Rusanov AL, Luzzgina NG, Lisitsa AV. Sodium dodecyl sulfate cytotoxicity towards HaCaT keratinocytes: comparative analysis of methods for evaluation of cell viability. Bull Exp Biol Med. 2017;163:284–288.
- [48] Terpiłowska S, Siwicka-Gieroba D, Siwicki AK. Cell viability in normal fibroblasts and liver cancer cells after treatment with iron (III), nickel (II), and their mixture. J Veterinary Res. 2018;62:535–542.
- [49] Fila G, Kasimova K, Arenas Y, et al. Murine model imitating chronic wound infections for evaluation of antimicrobial photodynamic therapy efficacy. Front Microbiol. 2016;7. doi:10.3389/fmicb.2016.01258.
- [50] Jantová S, Topol'ská D, Janošková M, et al. Original article. Study of the cytotoxic/toxic potential of the novel anticancer selenodiazoloquinolone on fibroblast cells and 3D skin model. Interdiscip Toxicol. 2016;9:106–112.